7th European Workshop on Structural Health Monitoring
July 8-11, 2014. La Cité, Nantes, France

DETECTION OF IMPULSE-LIKE AIRBORNE SOUND FOR DAMAGE IDENTIFICATION IN ROTOR BLADES OF WIND TURBINES

Thomas Krause, Stephan Preihs, Jörn Ostermann

Institut für Informationsverarbeitung, Leibniz Universität Hannover
Appelstr. 9A, 30167 Hannover, Germany

{krause, preihs, ostermann}@tnt.uni-hannover.de

ABSTRACT

Structural health monitoring systems can help to improve safety and minimize the numerous economical burdens of wind turbines. To detect damage of rotor blades, several research projects focus on an acoustic emission approach. Acoustic emission stands for stress waves emitted by a damage process. For this approach components of the waves are measured with sensors mounted on the surface of the blade. Small damages can be detected, but the amount of sensors is relatively high due to the size of modern blades and high internal damping of composite materials.

The damage process and stress waves also emit airborne sound. In contrast to existing approaches we use the airborne sound for damage detection. We developed a detection algorithm based on our signal analysis which showed that airborne sound provides adequate features for cracking sound detection. We optimized and tested the algorithm with our airborne sound recordings of a full-scale rotor blade test. In the first three days of the long term fatigue test our algorithm detects nine events per day, 79% of the events are cracking sounds. In the remaining 73 days of the fatigue test the algorithm detects about one event per day.

KEYWORDS : *acoustic emission, airborne sound, damage detection, rotor blade, wind turbine*

INTRODUCTION

There are several publications of non destructive damage detection methods used for detecting damage in rotor blades of wind turbines. An overview can be found in [1] [2]. There are two rotor blade monitoring systems on the market [3] which mainly use a modal analysis approach. For detecting damage more reliably and in early stages many research projects focus on the acoustic emission approach. The aim of this approach is to detect components of the stress wave caused by the damage process. For this sensors mounted on the surface of the blade are used. With this approach small damages can be detected [1] [2] [4] [5]. The amount of sensors is relatively high due to the size of modern blades and high internal damping of composite materials [4] [5]. In addition using acoustic emission for damage detection in an operating wind turbine is an unsolved problem. The increase of the risk of damage from lightning strikes caused by the electrical conductive wires is the main problem which prevents testing an acoustic emission approach in an operating rotor blade. So far there are only few results published of using an acoustic emission approach in an operating wind turbine [6] [7].

The damage process and the resulting stress wave also emit airborne sound waves. We focus on using these airborne sounds. Surprisingly there are so far no published research results using airborne sound for rotor blade damage detection, even though we and others observed audible cracking during rotor blade stress tests [8]. Fibre optic microphones can be used for recording sound inside a rotor blade. Their cords are electrical isolating so they do not increase the risk of damage from lightning strikes. This makes the approach applicable in an operating wind turbine.

One well known application where airborne sound is processed and detection methods are used is speech recognition. The airborne sound is also used for detecting gunshots. The sound of gunshots has an impulse-like characteristic which is similar to audible cracking sounds. It has been shown that gunshots can be detected with a high detection rate and low false positive detections using different signal processing algorithms [9] [10] [11] [12]. A correlation based detection approach, comparing the time amplitude signal with a template signal, is proposed in [9]. In [10] multiple time domain and spectral audio features were combined in a feature vector. In [11] correlation with a template signal and spectral features are both used. In [12] linear predictive coding coefficients and a correlation feature are used to achieve a high true positive rate and a low false positive rate at the same time.

Based on the good results of the different gunshot detection algorithms we developed an algorithm for cracking sound detection.

1. AUDIO FEATURE DETECTION ALGORITHM

A real-time capable detection algorithm was developed for detecting and roughly localizing specific impulse-like signals which represent the audible cracking in airborne sound recordings inside a rotor blade. The detection algorithm is based on the comparison of the input signal with a model of the cracking sound. The model describes a non-tonal sound with a sudden increase in power, a specific characteristic in the power over frequency at the beginning of the impulse and a model for the decrease in signal power over time.

We analysed more than 60 cracking sounds which occurred during a full-scale rotor blade stress test, described in Section 2.1. There are several characteristics all analysed cracking sounds have in common. In Figure 1 the power spectrogram of a cracking sound in the recordings of the fatigue test is shown as an example. The spectrogram represents signal power over time and frequency. The cracking sound is displayed in the marked area.

The first characteristic is the impulse-like increase in power which is displayed in Figure 1 at 0.63 seconds. The maximal power occurs in this time period which we refer to as first part of the impulse. After this there is an approximately exponential decrease in power over time. In Figure 1 the power is displayed in decibel, therefore the decrease is approximately linear. The power of every impulse is distributed over a wide frequency range, so the impulses are non-tonal. Depending on the impulse, the frequency where maximum power occurs can shift in a wide frequency range. In our recordings the

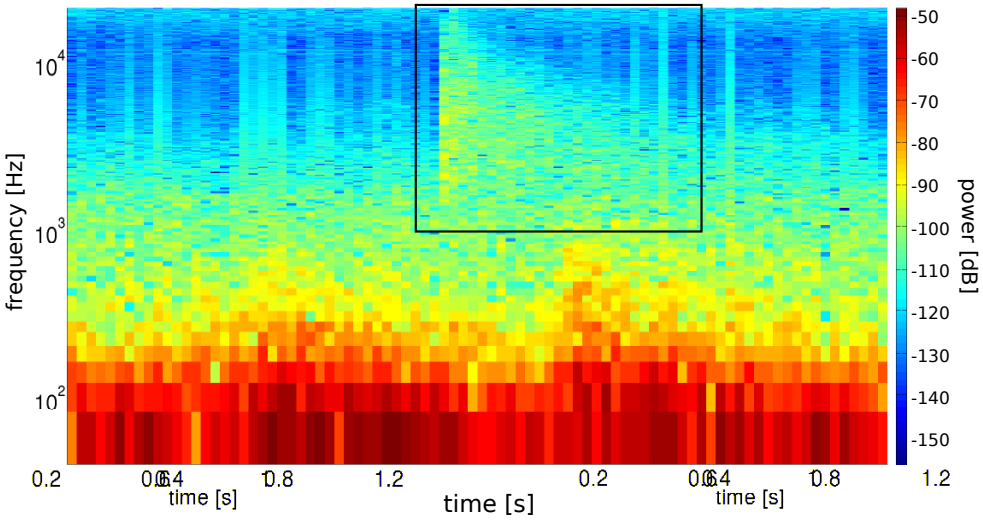

Figure 1 : Power spectrogram extract of the fatigue test with a detected cracking sound.

value occurs in the range of 150 Hz to 10 kHz. The cracking sound in Figure 1 has its maximum power at 2.2 kHz. Depending on the impulse the power also varies. The main characteristic of all impulses is a specific decrease in power toward higher frequencies. The decrease is linear in decibel with an approximately constant slope.

To represent the characteristics of the cracking sounds, five audio features were designed and used. The values of these features are calculated from the input signal. Threshold parameters $\delta_{i,min}$ $\delta_{i,max}$ are used for all i features to check if the signal is similar to the described model of the audible cracking.

1.1 Audio Features

1.1.1 Power Spectrogram

In a first step a power spectrogram of the signal is calculated. For this the discrete time amplitude signal $s(n)$ is transformed into a discrete short time Fourier transform $S_k(l)$ with overlapping windowed time chunks by

$$S_k(l) = \sum_{n=0}^{N_{FT}-1} s\left(n + l \cdot N_{hop}\right) w(n) e^{-j\frac{2\pi nk}{N_{FT}}} \quad \text{where} \quad 0 \leq k \leq N_{FT} - 1. \tag{1}$$

Here l is the resulting time index and k the resulting frequency index. A hamming window $w(n)$ is used with the same length as the transformation length N_{FT}. The parameter N_{hop} is half of the length of N_{FT}, such that the time chunks are half overlapped. The power spectrogram $P_k(l)$ is calculated using the squared absolute value and a normalization according to

$$P_k(l) = \frac{1}{N_{FT} \sum_{n=0}^{N_{FT}-1} |w(n)|^2} |S_k(l)|^2 \quad \text{for} \quad k = 0 \text{ und } k = \frac{N_{FT}}{2} \tag{2}$$

$$P_k(l) = \frac{2}{N_{FT} \sum_{n=0}^{N_{FT}-1} |w(n)|^2} |S_k(l)|^2 \quad \text{for} \quad 0 < k < \frac{N_{FT}}{2}. \tag{3}$$

1.1.2 Power Slope Feature

The first feature calculated and checked by the algorithm is the power slope of the signal. This feature reflects the impulse-like characteristic of a signal. The slope of the power $f_1(l)$ is calculated as follows:

$$f_1(l) = 10 \cdot \log_{10} \left[\sum_{k=k_b}^{k_e} P(k,l) - P(k,l-l_r) \right]. \tag{4}$$

In Formula 4 the raising time of the impulse model is denoted by l_r. The frequency bandwidth is specified by the parameters k_b and k_e. The parameters were set to leave out very low frequencies which contain high power and do not correlate with the cracking sound. The slope must exceed the value $\delta_{1,min}$ to conform to the model of the cracking sound. In this case an impulse might have its maximum power at the time l_c.

1.1.3 Noise Reduction

In case a power slope according to the model is observed we reduce the influence of not impulse-like signals in the power spectrogram using spectral subtraction. The assumption for spectral subtraction is a stationary signal. This assumption is approximately true if a short time period is taken. The signal model specifies that the rise time of the power is shorter than the decay time. Therefore the subtracting

spectrum is taken short time before the start of the impulse, at the time $l_c - l_r - 1$. The noise reduced spectrogram P_s is only used in the first part of the impulse and is calculated as follows:

$$P_s(k,l_c) = 10 \cdot \log_{10}\left[P(k,l_c) - P(k,l_c - l_r - 1)\right]. \tag{5}$$

1.1.4 Tonality Feature

There are three features calculated using the noise reduced power spectrum of the first part of the impulse. The first feature represents the tonality of the signal. For this the spectral flatness measure [13] the geometric mean of the power spectrum is divided by the arithmetic mean as

$$f_2(l_c) = \frac{\left(\prod_{k=k_b}^{k_e} P_s(k,l_c)\right)^{\frac{1}{k_e-k_b}}}{\frac{\sum_{k=k_b}^{k_e} P_s(k,l_c)}{k_e-k_b}}. \tag{6}$$

A value between zero an one is given where zero represents a maximal tonal signal and one a maximal noise-like signal. The impulse model is a non-tonal sound so the feature value should not be lower than the threshold $\delta_{2,min}$.

1.1.5 Spectrum Slope Feature

The second feature using the noise reduced power spectrum of the first part of the impulse is the slope of the power spectrum. For this the actual slope $f_3(l_c)$ of the simple linear regression is calculated as an approximation of the signal slope by

$$f_3(l_c) = \frac{\sum_{k=k_p}^{k_z} \left(k - \overline{k}\right)\left(P_s(k,l_c) - \overline{P_s(l_c)}\right)}{\sum_{k=k_p}^{k_z} \left(k - \overline{k}\right)^2}. \tag{7}$$

The power spectrum of the impulse model is characterized by a specific linear decrease in decibel from the frequency with maximal power k_p towards higher frequencies. For the frequency k_z the noise of the measurement system must be taken into account if the signal level is low in the higher frequencies. Here the overbar is the arithmetic mean from k_p to k_z. The upper and lower threshold parameter $\delta_{3,max}$ and $\delta_{3,min}$ define the allowable derivation from the characteristic slope of the model. In Figure 2 the power spectrum of a cracking sound in the first part of the impulse is displayed. In this Figure the slope of the model as well as the slope of the linear regression is shown.

1.1.6 Spectrum Similarity Feature

The third feature calculated using the noise reduced power spectrum of the first part of the impulse compares the impulse with the slope of the model. The power spectrum of the impulse model P_{prot} has a characteristic exponential decline of power towards higher frequencies. The representation of the signal in decibel linearises the decline. In Figure 2 the curve of the impulse model with the characteristic slope is given. The feature $f_4(l)$ measures the similarity of the signal spectrum and the model spectrum. The similarity is displayed in the euclidean distance normalized by the bandwidth of the spectrum by

$$f_4(l_c) = \frac{1}{k_z - k_p} \sqrt{\sum_{k=k_p}^{k_z} \left[P_{prot}(k) - P_s(k,l_c)\right]^2}. \tag{8}$$

The threshold parameter $\delta_{4,max}$ is the upper limit for a positive detection.

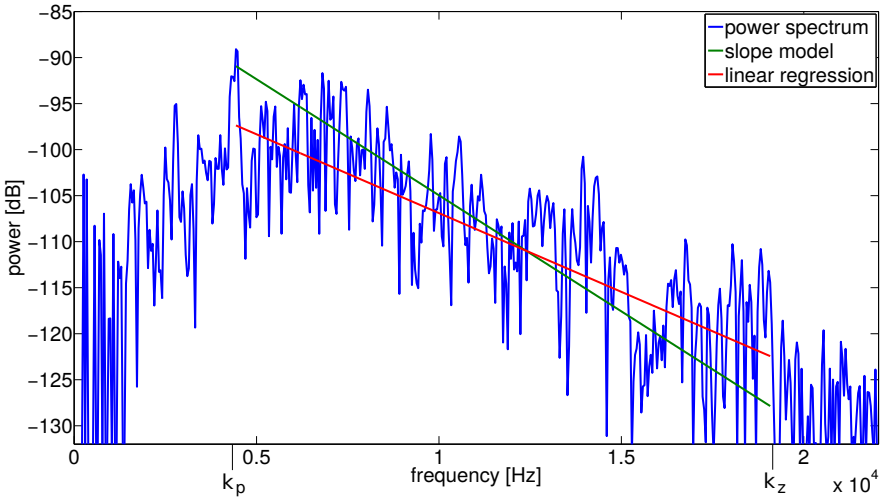

Figure 2 : Power spectrum of a cracking sound in the first part of the impulse.

1.1.7 Impulse Decay Feature

The decay of the impulse model has a linear decrease in signal power in decibel over time. The decay of the signal $f_5(l)$ is calculated using the power over time signal in the frequency k_p. The time period starts at the time index l_c. The length of the time period can be adjusted with the value l_d. The noise of the system has to be taken into account for this value. The decay of the signal is approximated calculating the slope of the simple linear regression by

$$f_5(l_c) = \frac{\sum_{l=l_c}^{l_c+l_d} \left(l-\bar{l}\right)\left(10\cdot\log_{10}\left(P(k_p,l)\right) - \overline{10\cdot\log_{10}\left(P(k_p)\right)}\right)}{\sum_{l=l_c}^{l_c+l_d}\left(l-\bar{l}\right)^2}. \tag{9}$$

Here the overbar is the arithmetic mean from l_c to l_c+l_d. An example of a cracking sound with the approximated decay is shown in Figure 3. The upper and lower threshold parameters $\delta_{5,max}$ and $\delta_{5,min}$ define the detection interval for this feature. In case the five features are detected at a time frame l_c the algorithm indicates that a cracking sound has occurred.

1.2 Localisation

The algorithm roughly localizes the detected impulses calculating a spherical latitude angle α. For the localisation a signal of a second microphone position is needed. The times of detection from both positions are computed to calculate the time difference t_{dif} of the detections. The assumption of a planar wave is used as a simplified model of the complex shape of the real sound waves in the rotor blade (Figure 4). The angle α is calculated by

$$\alpha = \arccos\left(\frac{t_{dif}\cdot c_{air}}{d_{mic}}\right). \tag{10}$$

The distance of the microphones is denoted by d_{mic} and the speed of sound by c_{air}. The angle is located on the axis through both microphone positions.

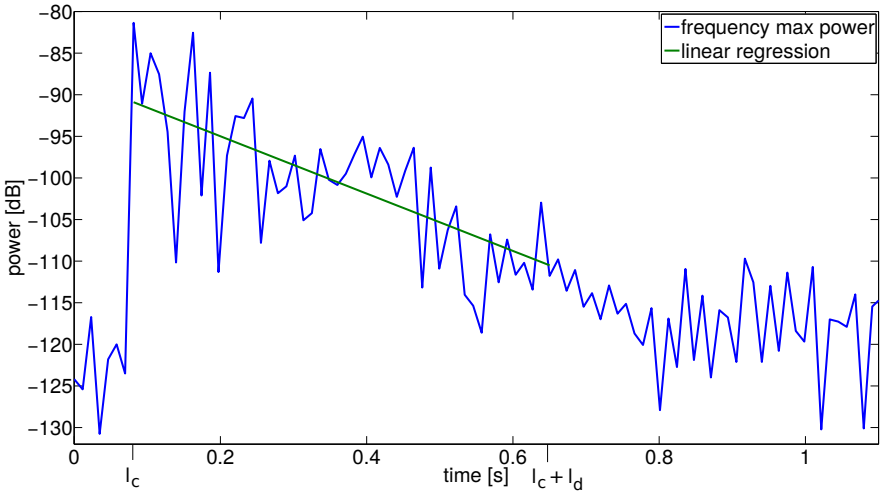

Figure 3 : Decay of power in the frequency band with maximum power.

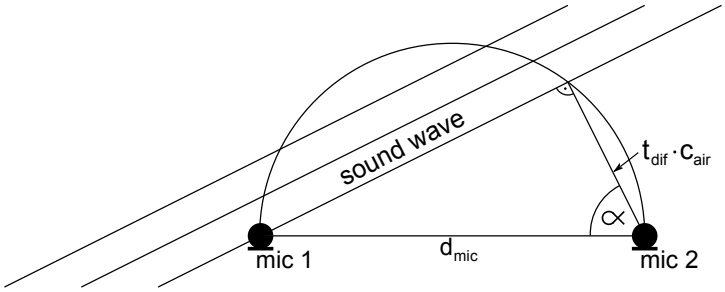

Figure 4 : Principle drawing for the localisation.

1.3 Flowchart

In Figure 5 the principal flow chart of the algorithm is shown. From the signal of one microphone the power spectrogram is calculated. Then the power slope feature is calculated and compared with the threshold $\delta_{1,min}$. If the slope is greater than $\delta_{1,min}$ the signal is further processed. In case of further processing the noise reduced power spectrogram is calculated. The remaining four features tonality, spectrum slope, spectrum similarity and impulse decay are calculated. If all this features are within the limits $\delta_{i,min}$ $\delta_{i,max}$, the algorithm detects a cracking sound for the current time index. Then the localisation is calculated using a signal from a second microphone position.

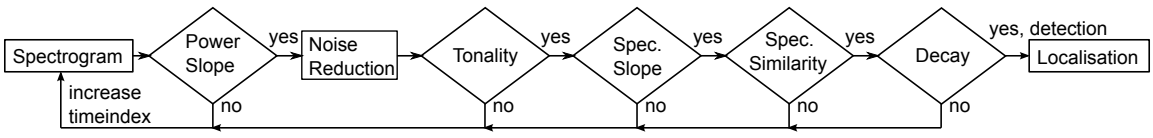

Figure 5 : Flow chart of the audio-feature algorithm.

2. RESULTS

2.1 Recordings During Rotor Blade Stress Tests

We recorded the airborne sound during parts of a certification test of a 55 m rotor blade. The recorded stress tests consisted of a flapwise fatigue test which took about two and a half months and four static tests which took about ten minutes each. Specifications of such tests can be found in [14].

The sound was measured at three different positions inside the rotor blade (Figure 6). The microphones were mounted on the spar facing toward the trailing edge. Three electrical microphones and one fibre optic microphone were used. The directionality of all microphones is specified as omnidirectional. The microphone signals were converted from analogue to digital with 44.1 kHz sampling rate and 24 bit precision. The digital data was saved losslessly as PCM files.

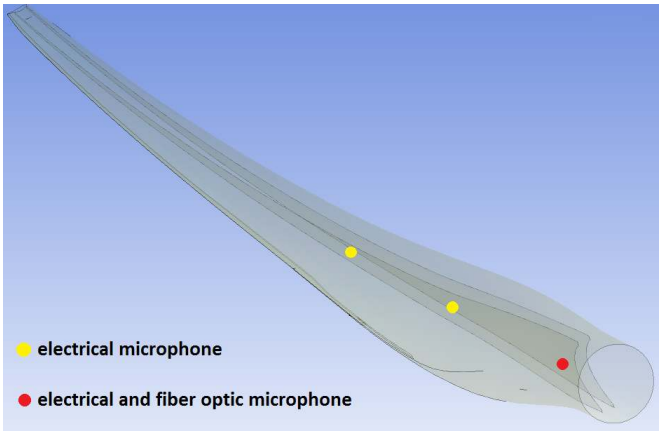

Figure 6 : Principle drawing of the microphone positions inside the rotor blade.

2.2 Results of the Detection Algorithm

The proposed audio-feature detection algorithm was tested and optimized using the recordings of the full-scale stress tests described in Section 2.1. Parts of the recordings were manually labelled and used as ground truth data for the statistical evaluation of the algorithm. The full data of the static rotor blade tests and more than ten hours of the fatigue test were labelled. This data was divided equally to get a training set and a test set. The fourier transformation length was set to 1024 samples. The thresholds and parameters of the algorithm were empirically optimised using the training set data.

The in the following given results have been achieved by processing the signal of the optical microphone. In the test set the algorithm achieves 49 true positive detections. For impulses with high power the sensitivity[1] is 86%. Impulses with low power are detected with an sensitivity of 44%. There are no false detections in the test set.

The algorithm was also used to analyse the whole fatigue test data, which consists of about two and a half months non-stop recordings. All positive detections were manually checked and labelled as false positive or as true positive detections. In the first three days of the long term fatigue test our algorithm detects nine events per day. 78,8% of these events are cracking sounds. In the remaining 73 days of the fatigue test about one event per day is detected. The false positive rate for the whole recordings, including the first three day, is 0.89 events per day.

In the recorded fatigue test no substantial structural damage occurred. Only in the beginning of our recordings the rotor blade adapted to the load with audible cracking sounds. After this the structure

[1] The sensitivity is the number of correctly identified impulses divides by all impulses in the set.

did not change much and no serious damage occurred. This led to rather few true positive detections in this time period.

CONCLUSION

In this paper, an algorithm for detection of cracking sounds in rotor blades of wind turbines is presented. It is based on five audio features which represent characteristics of a cracking sound model. The model describes a non-tonal sound with a sudden increase in power, a specific characteristic of the power over frequency at the beginning of the impulse and a model for the decrease in signal power over time. The algorithm employs a noise reduction method and roughly locates the detected sounds by processing two microphone signals.

We optimized and tested our algorithm with our airborne sound recordings of a full-scale rotor blade test. The analysis of the data shows promising results. In the first three days of the long therm fatigue test our algorithm detects nine events per day, 79% of the events are cracking sounds.

With this paper the idea using the airborne sound for rotor blade damage detection has taken a first step. The use of optical microphones makes this a promising approach for rotor blade structural health monitoring in operating wind turbines.

Our next step is a measurement campaign which includes a full-scale fatigue test where a rotor blade is tested till failure. These tests will be the basis for a further development of a rotor blade structural health monitoring system.

REFERENCES

[1] C. C. Ciang, J.-R. Lee, and H.-J. Bang. Structural health monitoring for a wind turbine system: a review of damage detection methods. *Measuement Science and Technology 19*, page 20 ff, 2008.

[2] P.J. Schubel, R.J. Crossley, E.K.G. Boateng, and et al. Review of structural health and cure monitoring techniques for large wind turbine blades. *RenewableEnergy*, 51:113–123, 2012.

[3] DNV GL SE. List of Certifications - Condition Monitoring Systems (CMS) / Monitoring Bodies for CMS. http://www.gl-group.com/pdf/Condition_Monitoring_System.pdf, march 2014.

[4] G. R. Kirikeraa, V. Shindea, M. J. Schulza, and et al. Damage localisation in composite and metallic structures using a structural neural system and simulated acoustic emissions. *Mechanical Systems and Signal Processing*, 21:280–297, 2007.

[5] A.G. Beattie. Acoustic Emission Monitoring of a Wind Turbine Blade During a Fatigue Test. In *35th Aerospace Sciences Meeting*, 1997.

[6] O. Ley and V.F. Godinez-Azcuaga. A wireless system for structural health monitoring of wind turbine blades. *Safety, Reliability, Risk and Life-Cycle Performance of Structures and Infrastructures*, pages 275–279, 2013.

[7] M.J. Blanch and A.G. Dutton. Acoustic Emission Monitoring of Field Tests of an operating Wind Turbine. *Key Engineering Materials Vols. 245-246*, pages 475–482, 2003.

[8] P. A. Joosse, M. J. Blanch, A. G. Dutton, and et al. Acoustic Emission Monitoring of Small Wind Turbine Blades. *Journal of solar energy engineering*, 124(4):446–454, 2002.

[9] A. Chacon-Rodriguez, P. Julian, L. Castro, and et al. Evaluation of gunshot detection algorithms. *IEEE Transactions on Circuits and Systems*, 58, 2011.

[10] G. Valenzise, L. Gerosa, M. Tagliasacchi, and et al. Scream and Gunshot Detection and Localization for Audio-Surveillance Systems. *IEEE Conference on AVSS*, 2007.

[11] I. L. Freire and J. A. Apolinario Jr. Gunshot detection in noisy environments. *International Telecommunications Symposium (ITS)*, 7, 2010.

[12] T. Ahmed, M. Uppal, and A. Muhammad. Improving efficiency and reliability of gunshot detection systems. *International Conference on Acoustics, Speech and Signal Processing (ICASSP)*, 2013.

[13] A.H. Gray and J.D. Markel. A spectral-flatness measure for studying the autocorrelation method of linear prediction of speech analysis. *IEEE Trans. Acoust. Speech Signal Process.*, 22:207–217, 1974.

[14] IEC 61400-23 TS Ed.1. Wind turbine generator systems – Part 23: full-scale structural testing of rotor blades, 2001.